Photomodulation Spectroscopy of Iodine-Doped Polyacetylene; Phase Transition from Soliton Lattice to Metal

E. Ehrenfreund, Z. Vardeny,[a] and O. Brafman
Department of Physics and Solid State Institute, Technion, Haifa 32000, Israel

R. Weagley
Xerox Webster Research Center, Webster, New York 14580

and

A. J. Epstein
Department of Physics and Department of Chemistry, Ohio State University, Columbus, Ohio 43210
(Received 27 June 1986)

Using the photomodulation technique for iodine (I_3^-)-doped polyacetylene, we have found spectroscopic evidence for an abrupt phase transition at 5% I_3^-. The transition is from the lightly doped phase best described as soliton lattice to the heavily doped metallic phase. The phase transition is characterized by gradual disappearance of the single photoinduced soliton band in the semiconducting phase and a sudden appearance of *two* correlated photoinduced absorption bands associated with photogenerated charged defects in the metallic phase.

PACS numbers: 71.30.+h, 72.80.Le, 78.50.−w

Recent interest[1-9] in doping of conjugated polymers has focused on the phase transition from a semiconducting phase in lightly doped polymers to a metallic phase in heavily doped samples. *Trans*-polyacetylene, $(CH)_x$, is unique among the class of conjugated polymers because of its well-known twofold ground-state degeneracy. The heavily doped metallic phase in *trans*-$(CH)_x$ exhibits[4,5] Pauli susceptibility characteristic of normal metals and high dc conductivity,[4,9] yet it also shows the doping-induced ir-active vibrations[2,4] (IRAV) characteristic of localized charges in dimerized semiconducting chains. The lightly doped phase, on the other hand, shows very little Pauli susceptibility[5,9] but the conductivity is relatively high.[9] It was early proposed[6] that the metallic state is the result of phase disordering of the incommensurate Peierls semiconductor. Subsequently, it was suggested[7] that the abrupt crossover is from a lattice of spinless charged solitons to a strongly coupled polaronic metal.

In this Letter, we report on our study of iodine-doped polyacetylene $[CH(I_3^-)_y]_x$ using the photomodulation technique to characterize the photoexcitations and the ground-state properties as a function of iodine-doping level y up to and beyond the metallic phase transition. In the lightly doped phase ($y \leq 4.5\%$) we found a single photoinduced absorption (PA) band associated with photogenerated charged solitons, whose strength decreases with y and completely disappears from the spectrum for $y = 4.5\%$. The heavily doped phase ($y \geq 5\%$), on the other hand, is characterized by *two* correlated PA bands associated with photogenerated charged defects, identified as charged bipolarons or polarons. The neutral PA band known to exist in undoped $(CH)_x$ shifts from 1.35 eV (for $y = 0$) to 1.85 eV (for $y = 5\%$). This shift indicates a gap increase of about 1 eV, which can be described by modeling of the semiconducting phase as a "soliton lattice." Our results confirm spectroscopically the phase transition at $y = 5\%$ from a soliton lattice to a metallic state.

Steady-state photomodulation was measured with a chopped (140 Hz) Ar^+-laser beam at 458 nm for the modulated excitation beam and an incandescent light source for the probe beam. The transmission T and the photomodulated changes ΔT were divided to give the induced absorption. The samples were thin films (thickness of about 2000 Å) of trans-$(CH)_x$ polymerized onto NaCl substrates and subsequently doped with iodine by the slow doping method.[9] The iodine concentration was derived by measurement of the sample conductivity.[4]

Figure 1 shows the photomodulation spectra of *trans*-$[CH(I_3^-)_y]_x$ at 20 K for $y = 0$, 1%, 3%, and 4.5%. The spectrum for the undoped sample [Fig. 1(a)] is composed of two electronic PA bands[10,11] which peak at 0.45 eV (LE) and 1.35 eV (HE) and three sharp features which were identified[12,13] as photoinduced IRAV. The HE PA band derives its strength from states above 1.55 eV where ΔT changes sign ("isosbestic point") and turns into photoinduced bleaching (PB) peaking at ~ 1.95 eV, i.e., at the maximum of the interband absorption.[11] The HE band is an intrinsic photoexcitation of the $(CH)_x$ chain produced by intrachain absorption, which has been proposed[10,11,14] as a bound neutral soliton-antisoliton pair. The LE PA band, the photoinduced IRAV, and the oscillations between 1.4 and 1.7 eV [Fig. 1(a)] belong to photogenerated charged solitons $s^{\pm}$.[10-13] $s^{\pm}$ are pho-

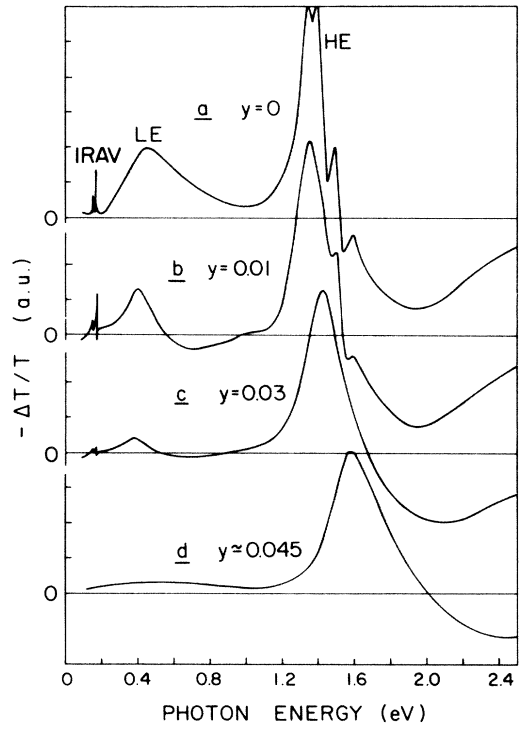

FIG. 1. Photomodulation spectra of *trans*-$[CH(I_3^-)_y]_x$ at 20 K for $y=0$, 1%, 3%, and 4.5%.

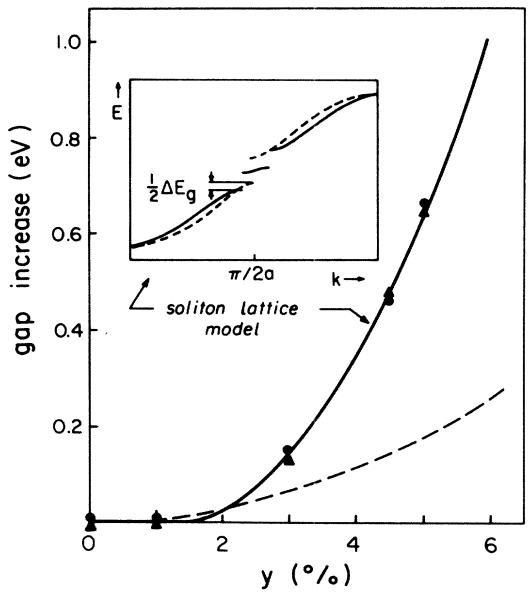

FIG. 2. The interband gap increase ΔE_g measured by the shifts of the isosbestic point (circles) and the maximum interband bleaching (triangles) as a function of y. The lines are calculations based on the SL model (solid line) and the frozen lattice model (dashed line). Inset: The schematic band structure for an undoped (dashed line) and doped (solid line) dimerized chain in the SL model.

toproduced mainly by interchain absorption, usually at the expense of native neutral-soliton (s^0) defects[15] which exist in undoped $(CH)_x$ samples with densities of $\sim 10^{19}$ cm^{-3}; formally the process can be written[11,15] as $2s^0 \rightarrow s^+ + s^-$. The evolution of the photomodulation spectrum with increasing y is shown in Figs. 1(b)–1(d). All spectral features associated with photogenerated $s^\pm$ weaken with increasing y while the HE band and the interband PB shift to higher energies with y, but remain strong. This supports that long-lived $s^\pm$ are extrinsically photogenerated,[15] and it also shows that the native s^0 defects become all charged[4] (by dopants) at $y \sim 4.5\%$.

Charged solitons $(s^+)_{dop}$ produced by iodine doping for $y < 3\%$ are characterized[9] by higher optical-transition energy (0.8 eV) than that of photogenerated $s^\pm$ (0.45 eV) and also by higher IRAV frequencies[15]: 900, 1285, and 1490 cm^{-1} for $(s^+)^2_{dop}$ compared to[12,13] ~ 500, 1280, and 1365 cm^{-1}, respectively, for $s^\pm$. The new PB band at 0.8 eV and the derivativelike shape at the IRAV energy range seen in Figs. 1(b) and 1(c) show therefore that there is an alternative channel for $s^\pm$ photogeneration in the lightly iodine-doped $(CH)_x$, namely,[15] $s^0 + (s^+)_{dop} \rightarrow s^+ + (s^0)_{dop}$. The optical transitions of s^0 and $(s^0)_{dop}$ are probably too close in energy and in any case they are covered by the much stronger HE band (Fig. 1). However, since the optical transitions for s^+ and $(s^+)_{dop}$ are very different, they can be easily identified[15] in Figs. 1(b) and 1(c) by the appearance of s^+ transitions at the expense of $(s^+)_{dop}$ transitions. This also explains the derivativelike shape of the IRAV where PB occurs at the high-frequency side.

If we focus on the interband transitions, Fig. 1 shows that the point of maximum bleaching in PB and the isosbestic point shift by the same amount towards higher energies with y. This is clear evidence that the interband optical gap (E_g) increases with doping. The increase ΔE_g, as measured by the shifts of the isosbestic point and the maximum bleaching, is plotted versus y in Fig. 2. The HE PA peak also shifts upward with y (Fig. 1). Experimentally, we found that the shift ΔE in the HE peak increases with y according to the relation $\Delta E = \frac{1}{2}\Delta E_g$. This supports the previous hypothesis[10,11,14] that the HE band is due to optical transitions of s^0 since s^0 energy level scales with $\frac{1}{2}E_g$, rather than with the full E_g.

To understand the doping-induced gap increase we perform two calculations. First, we do not allow for dimerization adjustments and calculate the increase ΔE_f for the onset of the modified interband transitions for a *frozen* dimerized chain. We find

$$\Delta E_f = [2\pi^2 t^2 / E_g(0)]y^2, \quad (1)$$

where $E_g(0)$ is the $y=0$ gap, t is the nearest-neighbor

transfer integral, and y is the doping concentration which is also the density of deoccupied states. The calculated $\Delta E_f(y)$ function [Eq. (1)] is shown in Fig. 2 as a broken line, where $t=2.5$ eV and $E_g(0)=1.7$ eV were taken as parameters representing undoped *trans*-$(CH)_x$. The calculations do not reproduce the data; $\Delta E_g(y)$ is considerably higher. It is therefore clear that $\Delta E_g(y)$ must be explained by allowing also dimerization adjustments to take place upon doping. Such calculations were done by the modeling of doped $(CH)_x$ as a soliton lattice (SL).

The SL self-consistent calculations have demonstrated[16-18] that (a) new subgap electronic bands are formed as a result of overlap between defect wave functions, and (b) the continuum bands are pushed apart[16] increasing the interband-transition onset more than by just band deoccupation. Although the calculations were performed on the assumption of an ordered doping pattern, it seems reasonable that the defect wave functions overlap, pushing apart the original gap even in dopant-disordered systems. In the SL model ΔE_g is given by[18]

$$\Delta E_g(y)=[\kappa(y)^{-1}-1]E_g(0), \qquad (2)$$

where $\kappa(y)$ is determined by the relation $\kappa K(\kappa y 2\zeta/a)=1$. Here $K(x)$ is a complete elliptic integral, a is the mean intercarbon distance projected along the chain, and ζ is the soliton coherence length. The SL band scheme[18] is depicted in the inset of Fig. 2. Assuming $2\zeta=15a$, we plot $\Delta E_g(y)$ calculated from Eq. (2) as a solid line in Fig. 2. The SL model (which neglects electron correlations) is a remarkably accurate fit to the data points. This shows that (a) the lightly doped semiconducting phase can be well described in terms of SL, and (b) electron correlations are not important for doped $(CH)_x$, probably because of screening caused by the doping induced charges.

The transition to the metallic phase at $y\sim 5\%$, which is ordinarily measured by a rapid increase in the magnetic susceptibility,[5] is observed here as a sharp downward shift in the doping-induced IRAV frequencies. Figure 3 shows the dependence of the highest doping-induced IRAV frequency upon y; it was obtained by ir absorption with a resolution of 4 cm^{-1} with our experimental setup for measuring T. An abrupt decrease from 1385 to 1360 cm^{-1} is readily observed at $y\sim 5\%$. Similar results were measured for the lowest doping-induced IRAV frequency,[19] which changes from ~ 900 cm^{-1} for $y=1\%$ to ~ 400 cm^{-1} for $y=6\%$. The variation in the IRAV frequencies can be translated to variation in the pinning parameter α_p using the amplitude-mode formalism[20]; this is shown in Fig. 3. The decrease in α_p with y shows that $(s^+)_{dop}$ are less pinned with increasing doping. Since α_p is proportional to the second derivative of the potential energy[20] describing $(s^+)_{dop}$ in the electrostatic field of I_3^-, its drop for $y\sim 5\%$ may be explained by additional screening which indicates a transition to a metallic phase.

The photomodulation spectrum of *trans*-$[CH(I_3^-)_{0.05}]_x$ in the metallic phase is shown in Fig. 4 for two laser excitation intensities I_L. Compared to the spectrum of $y=4.5\%$ [Fig. 1(d)] just below the phase transition, Fig. 4 shows *two new* electronic PA bands: B_1 at ~ 0.1 eV and B_2 at ~ 1.9 eV, and the photoinduced IRAV reappear. The two PA bands and

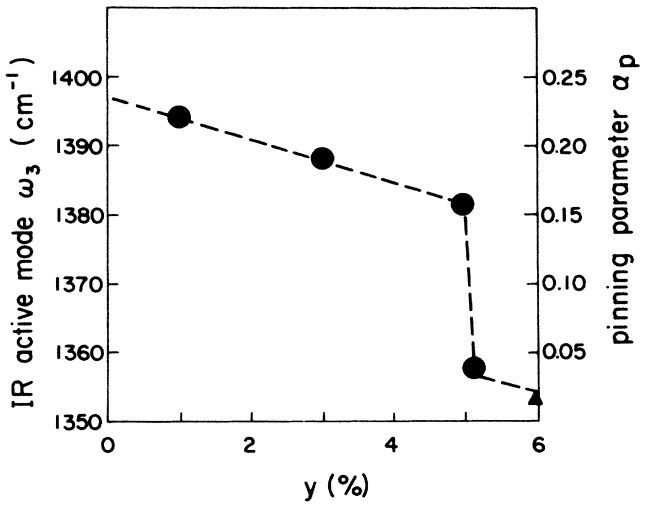

FIG. 3. The highest doping-induced IRAV frequency as a function of y. The right-hand scale gives the calculated pinning parameter for the charged defect.

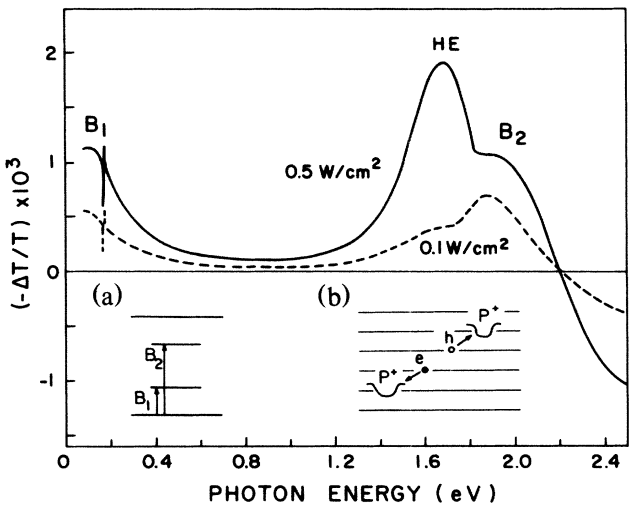

FIG. 4. Photomodulation spectra of *trans*-$[CH(I_3^-)_{0.05}]_x$ in the metallic phase for two excitation intensities. Inset (a): Energy levels and optical transitions for a positively charged bipolaron. Inset (b): Possible interchain photogeneration of bipolarons in a polaronic metal.

the IRAV are correlated. Their intensities increase as $I_L^{1/2}$ (see Fig. 4), and they decrease together with increasing temperature. This shows that the two PA bands and the IRAV belong to the same photogenerated defect, which therefore is charged, has bimolecular recombination kinetics, and is characterized by *two* strong optical transitions. The HE PA band which also appears in the spectrum depends linearly on I_L (Fig. 4) and therefore does not result from the photogenerated charged defect. We propose that the HE band is still photoproduced by intrachain absorption, while the long-lived charged defects are generated by interchain absorption as schematically shown in Fig. 4, inset (b). The relatively strong PA bands are the signature[21] of polarons or bipolarons, and therefore we identify the photoinduced defects as charged polarons or bipolarons.

The coexistence of subgap PA bands and IRAV characteristic of localized defects in semiconductor conjugated chains rules out a simple metal for the heavily doped phase. Since the photoinduced IRAV spectrum consists of absorption as well as bleaching (Fig. 4), we conclude that the metallic-phase ground state contains a varying order parameter: incommensurate charge-density wave (ICDW),[6] charged solitons, polarons, or bipolaron arrays. The large paramagnetic susceptibility[4,5] observed for $y \sim 5\%$ rules out spinless charged-defect arrays such as solitons or bipolarons and therefore the disordered ICDW model[6] or the "polaronic metal" model[7] is in agreement with our findings. Interchain photoexcitation in the ICDW model forms polarons P^+ and P^- with two energy levels, in the gaps between the ICDW band and the valence and conduction bands, respectively. B_1 and B_2 transitions in this case are the two strong transitions of polarons[21]; a third transition is expected[21] to be very weak. For the polaron-metal model[7] the ground state contains an array of polaroniclike distortions. Interchain photoexcitation may create bipolarons [Fig. 4, inset (b)] via the reaction $2P^+ \rightarrow BP^{++} + PB^0$, where the electron annihilates a positive polaron and the hole creates a doubly charged defect (BP^{++}). The two bipolaron transitions are depicted in Fig. 4, inset (a); however for this case B_2 is expected[21] to have much lower oscillator strength than B_1. To distinguish between these two proposed models one must have additional information about the interchain photoexcitations, such as their spins, which can be obtained by light-induced ESR measurements. Such measurements were not done at this time.

In conclusion, *trans*-$[CH(I_3^-)_y]_x$ shows two optically distinctive regions with a transition at $y = 5\%$. The ground state and the photoexcitations in the semiconducting phase are well described by the soliton-lattice model. The long-lived interchain photoexcitations in the metallic phase are polarons or bipolarons.

The work was supported in part by the U.S.–Israel Binational Science Foundation, Jerusalem, Israel, and by the Israeli Academy for Basic Research, Jerusalem, Israel.

[a]Present address: Division of Engineering, Box D, Brown University, Providence, RI 02912.

[1]C. K. Chiang *et al.*, Phys. Rev. Lett. **39**, 1098 (1977).
[2]J. F. Rabolt, T. C. Clarke, and G. B. Street, J. Chem. Phys. **71**, 4614 (1979).
[3]A. J. Epstein *et al.*, Solid State Commun. **38**, 683 (1981).
[4]A. J. Epstein *et al.*, J. Phys. (Paris), Colloq. **44**, C3-1497 (1983); A. J. Epstein *et al.*, Mol. Cryst. Liq. Cryst. **117**, 147 (1985).
[5]J. Chen, T. C. Chung, F. Moraes, and A. J. Heeger, Solid State Commun. **53**, 757 (1985).
[6]E. J. Mele and M. J. Rice, Phys. Rev. B **23**, 5397 (1981).
[7]S. Kivelson and A. J. Heeger, Phys. Rev. Lett. **55**, 308 (1985).
[8]B. Horovitz, Phys. Rev. Lett. **55**, 1429 (1985).
[9]A. J. Epstein *et al.*, Phys. Rev. Lett. **50**, 1866 (1983).
[10]J. Orenstein and G. L. Baker, Phys. Rev. Lett. **49**, 1043 (1982).
[11]Z. Vardeny, E. Ehrenfreund, and O. Brafman, Mol. Cryst. Liq. Cryst. **117**, 245 (1985).
[12]Z. Vardeny, J. Orenstein, and G. L. Baker, Phys. Rev. Lett. **50**, 2032 (1983).
[13]G. B. Blanchet, C. R. Fincher, and A. J. Heeger, Phys. Rev. Lett. **50**, 1938 (1983).
[14]S. Kivelson and W. K. Wu, Bull. Am. Phys. Soc. **31**, 330 (1986), and to be published.
[15]J. Orenstein *et al.*, Phys. Rev. B **30**, 786 (1984).
[16]J. L. Bredas *et al.*, Phys. Rev. B **29**, 6761 (1984).
[17]S. A. Brazovskii, S. Gordyunin, and N. N. Kirova, Zh. Eksp. Teor. Fiz. **31**, 485 (1980) [JETP Lett. **31**, 456 (1980)].
[18]B. Horovitz, Phys. Rev. Lett. **46**, 742 (1981).
[19]X. Q. Yang *et al.*, Mol. Cryst. Liq. Cryst. **117**, 267 (1985).
[20]B. Horovitz, Solid State Commun. **41**, 720 (1982).
[21]K. Fesser, A. R. Bishop, and D. K. Campbell, Phys. Rev. B **27**, 4804 (1983).